International Journal of Pharmaceutics, 64 (1990) 7–25
Elsevier

IJP 02142

Quantitation of simultaneous diffusion and metabolism of β-estradiol in hairless mouse skin: Enzyme distribution and intrinsic diffusion/metabolism parameters

Puchun Liu [1], William I. Higuchi [1], Abdel-Halim Ghanem [1], Tamie Kurihara-Bergstrom [2] and William R. Good [1,2]

[1] *Department of Pharmaceutics, University of Utah, Salt Lake City, UT 84112 (U.S.A.) and* [2] *Pharmaceuticals Division, Ciba-Geigy Corporation, Ardsley, NY 10502 (U.S.A.)*

(Received 20 June 1989)
(Modified version received 28 February 1990)
(Accepted 28 February 1990)

Key words: β-Estradiol; Hairless mouse skin; Diffusion; Metabolism; Biophysical model; Enzyme distribution; Intrinsic parameters

Summary

This paper describes a systematic experimental and theoretical study of the simultaneous diffusion and metabolism of β-estradiol ($E_{2\beta}$) in hairless mouse skin (in vitro). The strategy involved (a) considering a general three-layer skin model (stratum corneum, epidermis, and dermis), (b) considering three possible enzyme distributions (Model A: homogeneous enzyme distribution across both epidermis and dermis; Model B: homogeneous enzyme distribution in the epidermis; and Model C: homogeneous enzyme distribution in the 'basal cell layer' only of the epidermis), and (c) carrying out a wide range of independent diffusion experiments so that a 'best' model may be deduced in which all of the experimental data are consistent with the model and a single set of transport and metabolism parameters. The various diffusion/metabolism experiments included using three skin membranes (dermis, stripped skin, and full-thickness skin), two membrane configurations (transport of permeants in the direction: stratum corneum → epidermis → dermis, and in the reverse direction), two permeants ($E_{2\beta}$ and estrone, E_1, the principal metabolite), and measuring three fluxes (forward fluxes of $E_{2\beta}$ and E_1 and the back flux of E_1). Analysis of all of the experimental data demonstrated that Model C was superior to Models B and A; within the uncertainties of the experiments and model fitting, Model C agreed well with the data in all instances while the predictions of Models B and A exhibited significant deviations from the experimental data.

Introduction

Transdermal and topical drug delivery research has often only focussed upon the diffusion aspects and ignored dermal metabolism. Recent evidence from in vitro and in vivo experiments has shown that cutaneous metabolism may significantly influence local drug action, toxicity and delivery through skin (Ando et al., 1977; Noonan and Wester, 1983, 1987; Bucks, 1984; Kao and Hall, 1987; Martin et al., 1987).

Quantification of the dermal metabolism behavior of a drug in the context of simultaneous transport and metabolism is important in any systematic approach to the design of drugs and drug formulations for dermal and transdermal applications. Most previous dermal metabolism studies have been of a rather descriptive nature, and a

Correspondence: W.I. Higuchi, Department of Pharmaceutics, University of Utah, Salt Lake City, UT 84112, U.S.A.

need exists for quantitative approaches for assessing the influence of dermal metabolism on dermal and transdermal drug delivery.

This paper describes a quantitative biophysical model approach to the mechanistic understanding of diffusion and concurrent metabolism of β-estradiol ($E_{2\beta}$) in hairless mouse skin. The strategy involved (a) considering a general three-layer skin model (stratum corneum, epidermis, and dermis), (b) considering three possible enzyme distributions as depicted in Fig. 1 (Model A: homogeneous enzyme distribution in epidermis and dermis, Model B: homogeneous enzyme distribution in the epidermis, and Model C: homogeneous enzyme distribution in the 'basal cell layer' of the epidermis only), and (c) carrying out a wide range of independent experiments so that a 'best' model may be deduced in which all of the experimental data may be consistent with the model and a single set of transport and metabolism parameters. The various transport/metabolism experiments included using three skin membranes (dermis, stripped skin, and full-thickness skin), two membrane configurations (transport of permeants in the direction: stratum corneum → epidermis → dermis, and in the reverse direction), two permeants ($E_{2\beta}$ and estrone, E_1, the principal metabolite), and measuring three fluxes (e.g., forward fluxes of $E_{2\beta}$ and E_1 and the back flux of E_1). The proposed procedures combine experiments and biophysical models in a unique way and provide the means for factoring out and quantifying the influences of diffusion, metabolism, and the enzyme distribution in the overall process.

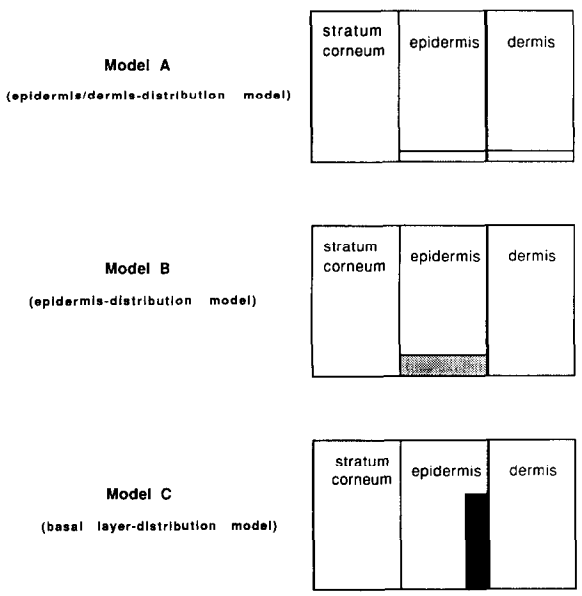

Fig. 1. Enzyme distribution models used in data interpretation.

Materials and Methods

Materials

[6,7-^{3}H]$E_{2\beta}$ (60.0 Ci/mmol) and [6,7-^{3}H]E_1 (51.8 Ci/mmol) were obtained in their ethanol solutions from New England Nuclear (Boston, MA). Further purification was carried out by HPLC with an associated fraction collector (see HPLC-FC-LSC identification-separation-assay method) until the radiochemical purity was in excess of 97%. The ethanol was evaporated with the aid of a nitrogen stream before [^{3}H]$E_{2\beta}$ or [^{3}H]E_1 was used for diffusion/metabolism experiments.

Unlabelled $E_{2\beta}$, E_1, estriol (E_3), and E_1-sulfate (Sigma, St Louis, MO) were used as standards in methanol (Baker, Phillipsburg, NJ). Normal saline (McGraw, Irvine, CA) was used for all experiments as a bulk phase solution. Analytical grade acetonitrile and diethyl ether (Baker) were used in the preparation of the HPLC mobile phase.

Skin preparations

A male hairless mouse, strain SKH-HR1, 12–15 weeks old (Temple University, Philadelphia, PA), was killed by spinal dislocation. Two pieces of the skin preparation were obtained from the abdominal region of each mouse. Three kinds of fresh membranes (full-thickness skin, stripped skin, and dermis) were prepared. Full-thickness skin, consisting of stratum corneum, viable epidermis and dermis, was obtained freed from adhering fat and other debris. Stripped skin, consisting of the epidermis and the dermis, was obtained after the stratum corneum was removed by a cellophane tape (Scotch tape, 3M Co., St. Paul, MN) stripping technique (Yu et al., 1979b). Dermis was obtained by removing the epidermal half of the

skin by using a dermatome (Yu et al., 1979b). The dermis thickness was measured with a micrometer before and after the experiment by sandwiching the membrane between two glass slides (Yu et al., 1979b).

A stripped skin homogenate supernatant was prepared by homogenizing the minced and weighed stripped skin tissue in a homogenizer tube (Bellco Glass, Vineland, NJ) for about 5 min with an appropriate amount of PBS (phosphate buffer solution, pH 7.3) to give a 10% homogenate. The homogenate was centrifuged for 5 min at 3000 rpm in a microcentrifuge. The sediment was resuspended, rehomogenized, and centrifuged again, and this procedure was repeated for a total of three times. All of the above steps were carried out at about 4°C.

HPLC-FC-LSC identification-separation-assay method

Quantitative and qualitative analyses of $E_{2\beta}$ and its metabolites were performed by interfacing an HPLC (high-performance liquid chromatograph) with a fraction collector. Each fraction was analyzed by liquid scintillation counting. Fig. 2 is a flow diagram for the separation of estrogens and their metabolites by the HPLC-FC (fraction collector)-LSC (liquid scintillation counting) system.

The HPLC system was a V4 Variable-Wavelength Absorbance Detector (ISCO, Lincoln, NE), a 110B Solvent Delivery Module (Beckman Institute, San Ramon, CA), and a C6W injector (Valco Institute, San Antonio, TX). The species were resolved by a reversed-phase column, Resolvex C18 (10 μm), 250 × 4.6 mm (Fisher, Pittsburgh, PA) with acetonitrile-water (35 : 65)-diethyl ether (90 : 10) at a wavelength of 280 nm. $E_{2\beta}$ and its metabolites were separated and identified by comparing their retention times to those of known standards. After specific metabolites were identified, the radioactive samples were mixed with the non-radioactive standard mixture solution to give the HPLC chromatograms. Radioactive fractions were collected on a FOXY Fraction Collector (ISCO, Lincoln, NE) with mode 3 and cycle 0. The fraction collector was programmed to give fraction sizes based on the peak signals from the ISCO detector with a built-in peak separator. 10 ml of scintillation fluid (Ready-Solv CP, Beckman) was transferred into each fraction vial for scintillation counting (Beckman LS 750). An automatic quench correction curve programmed into the counter converted the cpm into dpm, which were then converted into concentration units.

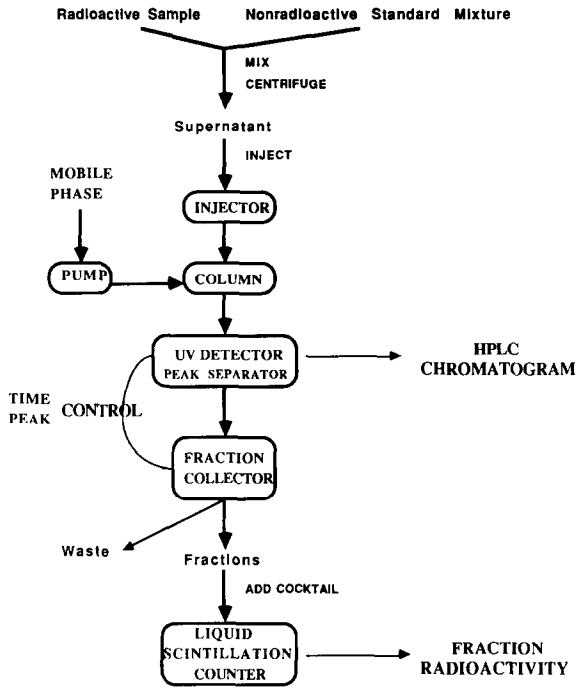

Fig. 2. Flow diagram for identification-separation-assay of [^{3}H]$E_{2\beta}$ and its metabolites by a HPLC (high-performance liquid chromatograph)-FC (fraction collector)-LSC (liquid scintillation counting) procedure.

Two-chamber cell diffusion / metabolism experiments

A diffusion cell (Durrheim et al., 1980) consisted of two half chambers, each having a volume of 2 ml and an effective diffusional area of about 0.7 cm^2. In each chamber, a stainless-steel (Carpenter stainless type 316L) stirrer with a small stainless-steel propeller was driven by a 150 rpm constant-speed motor. The thickness of an aqueous diffusion layer for a 150 rpm system was found to be 0.010 cm from a benzoic acid dissolution rate experiment (Yu et al., 1979b). The aqueous permeability coefficients of $E_{2\beta}$ and E_1 for this diffusion layer were then estimated to be around 1.1×10^{-3} cm/s.

The skin membranes (full-thickness skin, stripped skin, or dermis membrane) were sandwiched between the half cells and clamped. Two ml of normal saline were pipetted into both the donor and receiver chambers and allowed to equilibrate for 10 min at 37 °C. A predetermined level of the tritium-labelled solute ($E_{2\beta}$ or E_1) was added into the donor chamber and aliquots were withdrawn at predetermined time intervals after steady state was attained. In many of the experiments, 100-μl aliquots were taken from the receiver chamber and 10-μl aliquots from the donor chamber. The same volume of saline solution was added back to the receiver chamber to keep a constant volume. In the experiments with dermis and stripped skin, the donor solution was replaced at 1 h intervals to keep the donor permeant concentration constant (about 0.2 μg/ml $\pm$5%). The receiver chamber was always maintained under sink conditions ($\lesssim$ 10 % of the donor concentration). Except when taking a sample, the sample port was covered to avoid evaporation during the experimental period.

Incubation experiments with stripped skin homogenate

The reaction was started by adding 15 μCi (0.06 μg) of [^{3}H]$E_{2\beta}$ to 5 ml of either the homogenate or its supernatant of the stripped skin, prewarmed to 37 °C in a shaker/bath. Samples were taken at predetermined times and analyzed by the HPLC-fraction collector-scintillation counting procedure as previously described.

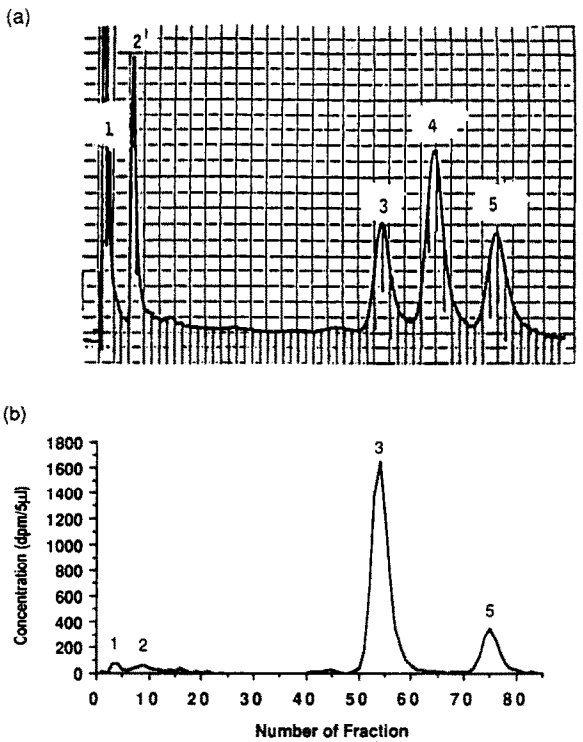

Fig. 3. Incubation of [^{3}H]$E_{2\beta}$ with supernatant of stripped skin homogenate. Peak identification: (1) E_1-sulfate (a representative of the aqueous conjugates), (2) E_3, (3) $E_{2\beta}$, (4) $E_{2\alpha}$, and (5) E_1. (a) HPLC chromatogram for separation of the nonradioactive $E_{2\beta}$ and its possible metabolites. (b) A typical chromatogram of a 2 h incubation sample of the supernatant containing [^{3}H]$E_{2\beta}$ and its possible ^{3}H-metabolites.

Results and Discussion

Incubation of $E_{2\beta}$ with stripped skin homogenate

Since there was no chemical degradation of $E_{2\beta}$ and E_1 in saline alone, all chemical changes were ascribed to enzymatic reactions. Metabolites formed by enzymes present in the skin were characterized from these incubation experiments. Fig. 3a shows an HPLC chromatogram for the separation of $E_{2\beta}$ and its possible metabolites: E_1, α-estradiol ($E_{2\alpha}$), estriol (E_3), and the aqueous conjugates (C). In order to resolve the two epimeric estradiols ($E_{2\beta}$ and $E_{2\alpha}$), diethyl ether was used as an organic modifier in the water-acetonitrile for the reverse-phase HPLC (Lee et al., 1981). Good separation of E_3 and C (E_1-sulfate as a representative) was also achieved in this system. Fig. 3b is a typical chromatogram of a 2 h sample from the incubation experiment of $E_{2\beta}$ with the stripped skin homogenate supernatant. Radioactivity for each fraction was determined. From Fig. 3a, E_1 was identified as the major metabolite of $E_{2\beta}$. These results are consistent with reported findings in the skin of man and other species (Frost et al., 1966; Weinstein et al., 1968; Longcope, 1980). 17β-Hydroxysteroid dehydrogenase, located in microsomes of rat skin, is an enzyme catalyzing the stereospecific interconversion of $E_{2\beta}$ and E_1 (Davis et al., 1972; Finnen et al., 1985).

The enzyme leaching problem was examined (Liu, 1989) and it was found that no significant enzyme leaching occurred from either the dermis side or the epidermis side of the stripped skin during the experiments.

Flux determination in the two-chamber diffusion cell experiments

Two-chamber cell diffusion/metabolism experiments were used to define the metabolism (A → B) aspects both qualitatively and quantitatively. The experiments with dermis were carried out first, followed by stripped skin and then full-thickness skin. Fig. 4 represents the typical experimental results with $E_{2\beta}$ as the permeant/substrate for all three skin membrane cases. At steady state, the following equations were used to calculate the forward fluxes for the drug ($J_{A,f}$) and for the metabolite ($J_{B,f}$) and the back flux for the metabolite ($J_{B,b}$):

$$J_{A,f} = \frac{\left(\frac{dA_{A,R}}{dt}\right)}{S} \quad (1)$$

$$J_{B,f} = \frac{\left(\frac{dA_{B,R}}{dt}\right)}{S} \quad (2)$$

$$J_{B,b} = \frac{\left(\frac{dA_{B,D}}{dt}\right)}{S} \quad (3)$$

where S is the effective diffusion area, $A_{A,R}$ is the drug amount in the receiver chamber, $A_{B,R}$ and $A_{B,D}$ are the metabolite amounts in the receiver and the donor chambers, respectively, and t represents time. In most situations, Eqns 1–3 may be employed in a rather straightforward manner. For example, according to Eqn 1, we may write

$$J_{A,f} = \frac{V_R\left(\frac{dC_{A,R}}{dt}\right)}{S} \quad (4)$$

where V_R is the volume of the receiver solution and $dC_{A,R}/dt$ is the change in the receiver solution concentration of A with time. Normally, Eqn 4 would be used (as in the present studies) under 'sink' conditions, i.e., where $C_{A,R} \ll C_{A,D}$ where $C_{A,D}$ is the steady-state donor concentration of A.

It can be shown (see Appendix A), however, that Eqns 1 and 4 may significantly underestimate $J_{A,f}$ even under sink conditions when dermis retention (or dermis 'holdup') is not negligible compared to the amount of A in the receiver chamber.

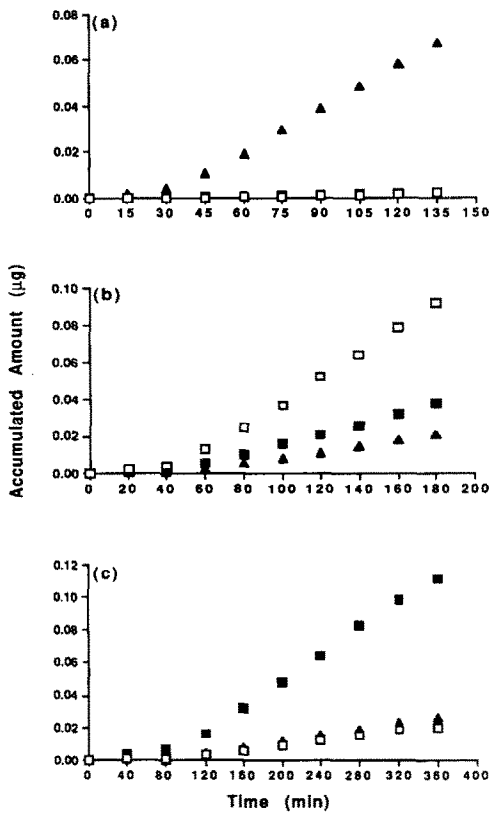

Fig. 4. Typical results from the two-chamber cell diffusion/metabolism experiment with $E_{2\beta}$ as the permeant/substrate: accumulated amounts (A_i) of $E_{2\beta}$ (▲) and E_1 (■) in the receiver and of E_1 in the donor (□) vs time for (a) dermis, (b) stripped skin (configuration 1), and (c) full-thickness skin (configuration 1). A_i was calculated from the chamber concentration at each time ($C_i, C_{i-1}, \ldots, C_2, C_1$), the chamber volume ($V$), and the sampling volume (V_s) as

$$A_i = C_i V + V_s(C_{i-1} + C_{i-2} + \ldots + C_2 + C_1)$$

In the experiments with dermis and stripped skin, the donor solution was replaced at 1-h intervals in order to maintain a constant donor concentration of the permeants (about 0.2 μg/ml ±5%). The receiver chamber was always kept under sink conditions (≲10% of the donor concentration).

In the present study, when $V_R = 2$ ml and when S, the area of the skin membrane, is around 0.70 cm^2, Eqn 4 may underestimate the correct $J_{A,f}$ by approx. 33% for full-thickness skin experiments and by approx. 25% for the dermis and stripped skin experiments. A procedure for correcting the flux values is described in Appendix A and has been applied where necessary to the experimental data.

Diffusion / metabolism experiments

$E_{2\beta}$ as the permeant / substrate. In this case where $E_{2\beta}$ is the substrate/permeant, $J_{A,f} = J_{2\beta,f}$ (the forward flux of $E_{2\beta}$), $J_{B,f} = J_{1,f}$ (the forward flux of E_1), and $J_{B,b} = J_{1,b}$ (the back flux of E_1). Table 1 summarizes the observed normalized fluxes determined in $E_{2\beta}$ diffusion/metabolism experiments with dermis, stripped skin, and full-thickness skin. Normalized fluxes are defined as the fluxes given by Eqns 1–3, divided by the donor concentration of the permeant/substrate.

No significant metabolism of $E_{2\beta}$ was found in the dermis experiments, indicating dermis is not a site for the enzymatic reaction. It is therefore concluded that the epidermis is the main site for the enzyme activity.

Results with stripped and full-thickness skin showed significant fluxes of E_1 (as the major metabolite) in the donor and receiver chambers. The flux ratio of metabolite $(J_{1,f} + J_{1,b})$-to-total $(J_{2\beta,f} + J_{1,f} + J_{1,b})$ was 0.73 to 0.85 for stripped skin and 0.84 to 0.97 for full-thickness skin. Metabolites other than E_1 were E_3 and C, the fluxes for which were less than 10% of those for E_1. For full-thickness skin, the forward $E_{2\beta}$ fluxes were essentially the same for the two configurations while the back flux of E_1 into the donor chamber in configuration 1 was much smaller than that in configuration 2, this being the case because the diffusion barrier of the stratum corneum was much greater than that of the dermis. For stripped skin, the total forward flux is relatively independent of configuration (configurations 1 and 2). The modest difference in back flux of E_1 between the two configurations is consistent with the enzyme being mainly located in the epidermis.

tbl IThe time-dependence of the enzyme activity was also considered in these experiments. The enzyme stability during the experimental period (< 6 h) was consistent with the fact that the concentrations of $E_{2\beta}$ and E_1 remained linear with time after steady state in all cases. This is in

TABLE 1

Observed normalized fluxes in diffusion / metabolism experiments with $E_{2\beta}$ as permeant / substrate using hairless mouse dermis, stripped skin, and full-thickness skin [a]

Skin membrane	Configuration [b]	Normalized flux ($\times 10^6$) (cm/s) [c]		
		$(J_{2\beta,f}/C_{2\beta,D})$	$(J_{1,f}/C_{2\beta,D})$	$(J_{1,b}/C_{2\beta,D})$
Dermatomed dermis (thickness: 225 ± 21 μm)	1	133.3 ±12.7	– [e]	– [e]
	2	119.0 ±13.4	– [e]	– [e]
Full-thickness dermis (thickness: 250 μm)	1	106.1 ±11.9 [d]		
	2	94.7 ±15.1 [d]		
Stripped skin	1	22.2 ± 7.73	42.3 ±12.8	82.6 ±24.3
	2	23.8 ± 8.51	39.1 ±10.5	26.0 ±10.3
Full-thickness skin	1	1.57 ± 0.33	7.01 ± 0.17	0.92 ± 0.24
	2	1.32 ± 0.20	7.14 ± 0.63	70.2 ±10.3

[a] Expressed as the mean ± S.D. ($n = 4$). Metabolites other than E_1 are E_3 and C. Compared to the flux for E_1, those for E_3 and C are less than 8 and 5% in stripped skin experiments and less than 5 and 4% in full-thickness skin experiments, respectively.

[b] Configuration 1: stratum corneum → epidermis → dermis; configuration 2: dermis → epidermis → stratum corneum.

[c] Normalized fluxes are defined as the fluxes divided by the donor concentration of the permeant/substrate.

[d] This number is the estimated full-thickness dermis permeability coefficient calculated from dermatomed dermis data using a correction factor (thickness of dermatomed dermis/thickness of full-thickness dermis).

[e] Fluxes for E_1 are about 3% of those for $E_{2\beta}$.

good agreement with our previous results on initial rate and long-term incubation experiments with the skin homogenate and its supernatant (Liu et al., 1986).

E_1 as the permeant/substrate. The results of the diffusion/metabolism experiments for E_1 as the substrate/permeant are reported in Table 2 where $J_{A,f} = J_{1,f}$, $J_{B,f} = J_{2\beta,f}$, and $J_{B,b} = J_{2\beta,b}$. Here $J_{1,f}$ and $J_{2\beta,f}$ have the same meaning as before and $J_{2\beta,b}$ is the back flux of $E_{2\beta}$. First, as was found with experiments using $E_{2\beta}$ as the substrate, there was very little enzyme activity in the dermis. This made possible the direct determination of the E_1 dermis permeability coefficient (with the thickness correction) which was found to be essentially the same as that for $E_{2\beta}$. With stripped and full-thickness skin, $E_{2\beta}$ was found as the major metabolite in the experiments with a relatively small flux ratio of metabolite $(J_{2\beta,f} + J_{2\beta,b})$-to-total $(J_{1,f} + J_{2\beta,f} + J_{2\beta,b})$, of 0.15 to 0.3 for stripped skin and of 0.3 to 0.7 for full-thickness skin.

Quantitative biophysical modelling

In the following, we will describe a quantitative biophysical model for the simultaneous diffusion and metabolism in the skin for the case where $E_{2\beta}$ is the permeant/substrate. The modelling techniques and the equations are similar to those discussed in the previous work (Yu et al., 1979a) on the transport and metabolism of vidarabine and its derivatives in hairless mouse skin; the reader is referred to this earlier work. Also, as was done previously, the first-order approximation for enzymatic reactions will be employed; this is a good approximation in the present studies where all of the substrate concentrations were at trace levels.

The model for hairless mouse skin is composed of n layers where n may be 3 or 4. In the steady state, we may write

$$D_{2\beta,i}\frac{d^2C_{2\beta}}{dx^2} - k_iC_{2\beta} = 0 \tag{5}$$

$$D_{1,i}\frac{d^2C_1}{dx^2} + k_iC_{2\beta} = 0 \tag{6}$$

The first term describes diffusion according to Fick's second law of diffusion. The second term represents the skin metabolism as a first-order reaction of $E_{2\beta} \rightarrow E_1$. The D terms are the diffu-

TABLE 2

Observed normalized fluxes in diffusion/metabolism experiments with E_1 as permeant/substrate using hairless mouse dermis, stripped skin, and full-thickness skin [a]

Skin membrane	Configuration [b]	Normalized flux ($\times 10^6$) (cm/s) [c]		
		$(J_{1,f}/C_{1,D})$	$(J_{2\beta,f}/C_{1,D})$	$(J_{2\beta,b}/C_{1,D})$
Dermatomed dermis (thickness: 218 ± 34 μm)	1	130.7 ± 20.6	– [e]	– [e]
	2	121.7 ± 18.0	– [e]	– [e]
Full-thickness dermis (thickness: 250 μm)	1	114.1 ± 15.2 [d]		
	2	106.2 ± 11.1 [d]		
Stripped skin	1	71.4 ± 19.6	14.2 ± 4.73	17.0 ± 7.23
	2	83.6 ± 31.9	8.63 ± 2.22	6.38 ± 1.94
Full-thickness skin	1	13.1 ± 2.02	4.95 ± 1.65	1.53 ± 0.43
	2	12.1 ± 3.50	2.73 ± 0.91	26.3 ± 9.06

[a] Expressed as the mean ± S.D. ($n = 3$). Metabolites other than $E_{2\beta}$ are E_3 and C. Compared to the flux for $E_{2\beta}$, those for E_3 and C are less than 10 and 8% in stripped skin experiments and less than 8 and 5% in full-thickness skin experiments, respectively.

[b] Configuration 1: stratum corneum → epidermis → dermis; configuration 2: dermis → epidermis → stratum corneum.

[c] Normalized fluxes are defined as the fluxes divided by the donor concentration of the permeant/substrate.

[d] This number is the estimated full-thickness dermis permeability coefficient calculated from dermatomed dermis data using a correction factor (thickness of dermatomed dermis/thickness of full-thickness dermis).

[e] Fluxes for $E_{2\beta}$ are about 2% of those for E_1.

sion coefficients and the k terms are the first-order enzyme rate constants. The C terms are the concentrations and the coordinate x ($0 \leq x \leq h$ (thickness)) is the depth in the membrane. The subscripts 2β and 1 refer to $E_{2\beta}$ and E_1 and i corresponds to the i-th layer of the skin. Full-thickness skin is then considered as a three-layer (stratum corneum, epidermis, and dermis) or a four-layer (stratum corneum, basal layer of epidermis, the remainder of the epidermis, and dermis) membrane as depicted by Model A, B, or C (see Fig. 1). The D and k, in general, may have different values for the different components of a membrane, but they are assumed to be constant within a particular membrane component or a subcomponent (see Model C discussion). The thicknesses are assigned values of 20, 20 and 250 μm for stratum corneum, epidermis, and dermis, respectively. For Model C, the basal layer will be assumed to be the lower one-third of the epidermis.

The fluxes (J) of $E_{2\beta}$ and E_1 at $x = x$ may be expressed as:

$$J_{2\beta}(x) = -D_{2\beta}\frac{dC_{2\beta}}{dx} \tag{7}$$

$$J_1(x) = -D_1\frac{dC_1}{dx} \tag{8}$$

We also have

$$\text{at } x = h,\ J_1 = J_{1,f} \text{ and } J_{2\beta} = J_{2\beta,f} \tag{9}$$

$$\text{at } x = 0,\ J_1 = -J_{1,b} \text{ and } J_{2\beta} = J_{2\beta,f} + J_{1,f} + J_{1,b} \tag{10}$$

Also, the boundary fractional concentrations are

$$\text{at } x = h,\ C_{2\beta} = 0 \text{ and } C_1 = 0 \tag{11}$$

$$\text{at } x = 0,\ C_{2\beta} = 1 \text{ and } C_1 = 0 \tag{12}$$

Eqns 5 and 6 may be solved analytically (Yu et al., 1979a, 1980b) or numerically (Hsu, 1981) with these boundary conditions as described below when the experimental flux data are available (see Appendix B). Computer iterations were performed to fit the calculated fluxes to the experimental data. Three parameters were adjusted in best fitting the data from each set of experiments to each model. The epidermis permeability coefficients for $E_{2\beta}$ and E_1 and the first-order enzyme rate constant were first simultaneously deduced using stripped skin experimental fluxes and the predetermined dermis permeability coefficients of $E_{2\beta}$ and E_1 (see Tables 1 and 2). Then these predetermined epidermis and dermis permeability coefficients were used with the full-thickness skin experimental fluxes to deduce simultaneously the 'best' value for the stratum corneum permeability coefficients of $E_{2\beta}$ and E_1 and the enzyme rate constant.

Experimental examination of the enzyme distribution models

The purpose of this section is to examine the three enzyme distribution models (Fig. 1) and to determine which one may best represent the experimental facts. A best model is that for which the experiments with different skin membranes and different configurations are consistent with the model and a single set of transport and metabolism parameters.

Firstly, Model A may be eliminated from further discussion as the experiments with dermis have led to the conclusion that there is little enzyme activity in the dermis (Tables 1 and 2). Therefore, the main question is: does Model B or C best represent the facts?

For Model B, data analysis has revealed important inconsistencies in a number of places (Table 3). The parameter values deduced from the different experiments show large variations in the case of Model B. Firstly, the four independent experiments have yielded significantly different values for the enzyme rate constant, k. Secondly, the permeability coefficient values for the two species in the epidermis and in the stratum corneum deduced from the best-fitting procedures show a large dependence upon the experimental configuration, and the differences are clearly outside the range of experimental uncertainties.

For Model C, however, the results of the independent experiments were found to be self-consistent within the framework of the model. As can

TABLE 3

Examination of Model B (epidermis-distribution model): diffusion and metabolism parameters deduced from Model B [a]

Parameter [b]	Stripped skin		Full-thickness skin		Average
	Configuration [c]		Configuration [c]		
	1	2	1	2	
k (s^{-1})	0.11 ± 0.02	0.66 ± 0.16	0.10 ± 0.03	0.30 ± 0.04	0.30 ± 0.30 [d]
$P_{2\beta,e}$ ($\times 10^4$) (cm/s)	7.61 ± 1.41	23.1 ± 9.60			15.4 ± 11.4 [d]
$P_{1,e}$ ($\times 10^4$) (cm/s)	0.21 ± 0.07 [e]	6.45 ± 1.82			3.33 ± 3.62 [d]
$P_{2\beta,s}$ ($\times 10^6$) (cm/s)			9.70 ± 3.15	2.12 ± 0.64	5.91 ± 4.64 [d]
$P_{1,s}$ ($\times 10^6$) (cm/s)			0.94 ± 0.29 [e]	9.52 ± 2.02	5.23 ± 4.88 [d]

[a] Expressed as the mean ± S.D. ($n = 4$) determined with dermis permeability coefficients of $E_{2\beta}$ and E_1: $P_{2\beta,d} = 1.0 \times 10^{-4}$ cm/s and $P_{1,d} = 1.1 \times 10^{-4}$ cm/s.

[b] k: first-order enzyme rate constant in the epidermis; $P_{2\beta,e}$ and $P_{1,e}$: epidermis permeability coefficient of $E_{2\beta}$ and E_1; $P_{2\beta,s}$ and $P_{1,s}$: stratum corneum permeability coefficient of $E_{2\beta}$ and E_1.

[c] Configuration 1: stratum corneum → epidermis → dermis; configuration 2: dermis → epidermis → stratum corneum.

[d] Significantly different.

[e] Out of the physically meaningful range.

be seen in Table 4, the best-fit values of the parameters deduced from the different experiments were the same within the experimental errors. The k values of about 0.70 s^{-1} were deduced from four different experiments. The epidermis permeability coefficients and the stratum corneum permeability coefficient for $E_{2\beta}$ and E_1 were deduced from two independent experiments, and the parameter values in each case were essentially the same. Table 5 shows the comparisons between the experimental data and the fluxes calculated with a single set of the parameters from Models B and C. All of these results collectively demonstrate that Model C described the results quite well and is clearly superior to Model B.

An examination of some of the model approximations and assumptions

A more complete consideration of the various metabolic pathways. The preceding model analysis for the case in which $E_{2\beta}$ was the permeant/substrate neglected metabolites other than E_1 and also neglected the back reaction of $E_1 \rightarrow E_{2\beta}$. Therefore, it would be instructive (a) to consider a more complete metabolism model for the case in which $E_{2\beta}$ is the permeant/substrate

TABLE 4

Examination of Model C (basal layer-distribution model): diffusion and metabolism parameters deduced from Model C [a]

Parameter [b]	Stripped skin		Full-thickness skin		Average
	Configuration [c]		Configuration [c]		
	1	2	1	2	
k (s^{-1})	0.82 ± 0.14	0.69 ± 0.15	0.70 ± 0.13	0.63 ± 0.18	0.71 ± 0.20
$P_{2\beta,e}$ ($\times 10^4$) (cm/s)	2.18 ± 0.43	1.99 ± 0.75			2.09 ± 0.73
$P_{1,e}$ ($\times 10^4$) (cm/s)	2.47 ± 0.86	2.16 ± 0.71			2.32 ± 0.73
$P_{2\beta,s}$ ($\times 10^6$) (cm/s)			9.42 ± 1.20	8.36 ± 1.91	8.89 ± 1.93
$P_{1,s}$ ($\times 10^6$) (cm/s)			10.8 ± 1.39	11.5 ± 2.53	11.1 ± 2.75

[a] Expressed as the mean ± S.D. ($n = 4$) determined with dermis permeability coefficients of $E_{2\beta}$ and E_1: $P_{2\beta,d} = 1.0 \times 10^{-4}$ cm/s and $P_{1,d} = 1.1 \times 10^{-4}$ cm/s.

[b] k: first-order enzyme rate constant in the epidermis; $P_{2\beta,e}$ and $P_{1,e}$: epidermis permeability coefficient of $E_{2\beta}$ and E_1; $P_{2\beta,s}$ and $P_{1,s}$: stratum corneum permeability coefficient of $E_{2\beta}$ and E_1.

[c] Configuration 1: stratum corneum → epidermis → dermis; configuration 2: dermis → epidermis → stratum corneum.

TABLE 5

Normalized fluxes in diffusion / metabolism experiments with $E_{2\beta}$ as permeant / substrate using hairless mouse skin membranes: comparisons between experimental and model calculations [a]

Configuration [b]	Skin	Normalized flux (cm/s)	Experiment	Model B	Model C
1	Stripped skin	$(J_{2\beta,f}/C_{2\beta,D}) \times 10^5$	2.22 ± 0.77	7.99 ± 4.47	2.96 ± 0.82
		$(J_{1,f}/C_{2\beta,D}) \times 10^5$	4.23 ± 1.28	6.67 ± 1.71	4.22 ± 1.15
		$(J_{1,b}/C_{2\beta,D}) \times 10^5$	8.26 ± 2.43	49.1 ± 9.55	10.3 ± 2.99
1	Full-thickness skin	$(J_{2\beta,f}/C_{2\beta,D}) \times 10^6$	1.57 ± 0.33	0.85 ± 1.00	1.54 ± 0.40
		$(J_{1,f}/C_{2\beta,D}) \times 10^6$	7.01 ± 0.17	5.49 ± 0.22	5.70 ± 1.65
		$(J_{1,b}/C_{2\beta,D}) \times 10^6$	0.92 ± 0.24	0.30 ± 1.00	0.57 ± 0.20
2	Stripped skin	$(J_{2\beta,f}/C_{2\beta,D}) \times 10^5$	2.32 ± 0.82	7.66 ± 4.66	2.58 ± 0.75
		$(J_{1,f}/C_{2\beta,D}) \times 10^5$	3.91 ± 1.05	1.24 ± 2.74	3.90 ± 1.10
		$(J_{1,b}/C_{2\beta,D}) \times 10^5$	2.60 ± 1.03	0.25 ± 1.05	1.75 ± 0.55
2	Full-thickness skin	$(J_{2\beta,f}/C_{2\beta,D}) \times 10^6$	1.32 ± 0.20	0.73 ± 1.08	1.49 ± 0.40
		$(J_{1,f}/C_{2\beta,D}) \times 10^6$	7.14 ± 0.63	4.38 ± 0.55	6.56 ± 1.92
		$(J_{1,b}/C_{2\beta,D}) \times 10^5$	7.02 ± 1.03	8.00 ± 1.00	6.61 ± 1.80

[a] Experimental data were copied from Tables 1 and 2. Model calculations were carried out with Models B and C. The single set of diffusion/metabolism parameters (average ± S.D.) in Table 3 were used for Model B calculations and those in Table 4 for Model C calculations.

[b] Configuration 1: stratum corneum → epidermis → dermis; configuration 2: dermis → epidermis → stratum corneum.

and (b) also to model the case for which E_1 is the permeant/substrate. The more general case has been numerically analyzed using the following equations for the basal cell layer in Model C with the three enzyme rate constants ($k_{2\beta\to1}$, $k_{1\to2\beta}$, and $k_{1\to3C}$ for the reactions of $E_{2\beta} \to E_1$, $E_1 \to E_{2\beta}$, and $E_1 \to E_3 + C$, respectively).

$$D_{2\beta}\frac{d^2C_{2\beta}}{dx^2} - k_{2\beta\to1}C_{2\beta} + k_{1\to2\beta}C_1 = 0 \qquad (13)$$

$$D_1\frac{d^2C_1}{dx^2} + k_{2\beta\to1}C_{2\beta} - (k_{1\to2\beta} + k_{1\to3C})C_1 = 0 \qquad (14)$$

$$D_{3C}\frac{d^2C_{3C}}{dx^2} + k_{1\to3C}C_1 = 0 \qquad (15)$$

where C_{3C} is the sum of the concentrations of E_3 and C and D_{3C} is the diffusion coefficient for E_3 and C. The stripped skin experimental fluxes for $E_{2\beta}$, E_1, and E_3 and C (Tables 1 and 2) from four different experiments ($E_{2\beta}$ and E_1 as the permeant/substrate in the two configurations) were used for this analysis with Model C by assuming the same permeability coefficient (or diffusion coefficient) for each species in dermis and epidermis. All of the transport parameter values used in the analysis were taken from Tables 1 and 4. Table 6 summarizes the results of this more complete analysis. First, the relative constancy of the rate constants from the different experiments again supports Model C as being most valid. Secondly, as anticipated, the effect of $k_{1\to2\beta}$, and $k_{1\to3C}$ together on the determination of $k_{2\beta\to1}$, is of the order of 10%. The conversion of $E_{2\beta}$ to E_1 is favored over the reverse reaction; this is in agreement with the reported in vivo work (Longcope and Williams, 1974). Finally, the $k_{2\beta\to1}$ values deduced from the E_1 experiments (Table 2) are in good agreement with those obtained from $E_{2\beta}$ experiments (Table 1).

Membrane thickness values used in the models. Although we have attempted to apply thickness values consistent with anatomy, the exact values assigned to the thickness for the stratum corneum, epidermis and dermis are not important because the permeability coefficients are the determined quantities in the present study. Thus, if a thick-

TABLE 6

A more complete consideration of the various metabolic pathways: analysis of Model C with stripped hairless mouse skin experimental fluxes [a]

Enzyme constant [b] (s^{-1})	$E_{2\beta}$ as substrate		E_1 as substrate		Mean ± S.D.
	Configuration [c]		Configuration [c]		
	1	2	1	2	
$k_{2\beta \to 1}$	0.93	0.78	0.74	0.73	0.80 ± 0.10
$k_{1 \to 2\beta}$	0.079	0.12	0.081	0.16	0.11 ± 0.040
$k_{1 \to 3C}$	0.0052	0.0010	0.0021	0.0018	0.0025 ± 0.0018

[a] The mean values of the fluxes in Tables 1 and 2 were used by considering the minor enzyme reactions of $E_1 \to E_{2\beta}$ and $E_1 \to E_3 + C$ with Model C where the enzyme is located mainly in the basal layer of the epidermis (near the dermo-epidermal junction) and with the same permeability coefficient for each species in dermis and in epidermis ($P_d = 1.1 \times 10^{-4}$ cm/s and $P_e = 2.2 \times 10^{-4}$ cm/s).

[b] First-order enzyme rate constant, $k_{2\beta \to 1}$, $k_{1 \to 2\beta}$, and $k_{1 \to 3C}$ for the reactions of $E_{2\beta} \to E_1$, $E_1 \to E_{2\beta}$, and $E_1 \to E_3 + C$, respectively.

[c] Configuration 1: stratum corneum → epidermis → dermis; configuration 2: dermis → epidermis → stratum corneum.

ness of 40 μm, instead of 20 μm, is assigned to the epidermis, then a diffusion constant that is 2-fold larger will be deduced. Also, if a thickness of 40 μm is used, an enzyme rate constant twice as large as that for the 20 μm case will be obtained; however, the total amount of enzyme per unit area of skin will be independent of the thickness assigned. For the stratum corneum and for the dermis, the actual values assigned for the thickness are also unimportant as long as the correct permeability coefficients are used.

Partition coefficient of unity for the epidermis and dermis. As the steady-state diffusion of $E_{2\beta}$, E_1, and many other permeants across stripped skin is well-approximated by a porous membrane model (Ghanem et al., 1987), the partition coefficient pertinent to the transport pathway should be an aqueous-to-aqueous partition coefficient. Physically, this may mean that permeants of different lipophilicity may have significantly different binding or partitioning tendencies to epidermis or dermis; however, because the binding/partitioning sites (other than the aqueous compartments) are apparently immobile sites, these do not contribute to steady-state permeant transport.

Diffusion coefficient gradient in the epidermis. The model calculations summarized in Table 3 (Model B) and Table 4 (Model C) assumed that the diffusion coefficient in the epidermis was constant. A key question has been whether some reasonable diffusion coefficient variation in the epidermis would permit satisfactory agreement between Model B and the experimental data. In order to examine this question, a quantitative simulation for the case of stripped skin was carried out by dividing the epidermis into two parts of equal thickness [near stratum corneum (Ns) and near dermis (Nd)] and assigning Nd-to-Ns diffusion coefficient ratios of 2, 10, and 50 for the two parts. It was felt that these calculations would represent a 'best case' scenario for Model B (especially with the ratio of 50). Table 7 represents an attempt to examine the experimental $E_{2\beta}$ results with stripped skin via the 'modified' Model B. It is shown that the deduced k values differ considerably between configurations 1 and 2, even when $D_{Nd}/D_{Ns} = 50$ which should be considered an extreme situation. Also, the deduced $D_{2\beta,Nd}$ and $D_{1,Nd}$ values generally show differences that are much too large at all D_{Nd}/D_{Ns} ratios. Because it was believed it would be instructive, similar calculations have been conducted using Model C. The results for the modified Model C are presented in Table 8. It is observed that the deduced k values differ much less between configurations 1 and 2 for all three D_{Nd}/D_{Ns} ratios (cf. results for modified Model B, Table 7). The modified Model C appears to describe the experimental fluxes best where the D_{Nd}/D_{Ns} ratio approaches 1.0, thus suggesting that Model C with no significant varia-

TABLE 7

Examination of modified Model B with stripped skin experiments of $E_{2\beta}$: diffusion and metabolism parameters deduced from the modified Model B [a]

D_{Nd}/D_{Ns}	Configuration [b]	k (s^{-1})	$D_{2\beta,Nd}$ (cm^2/s)	$D_{1,Nd}$ (cm^2/s)
2	1	0.15 ± 0.05	$(2.96 \pm 1.00) \times 10^{-7}$	$(1.60 \pm 0.50) \times 10^{-7}$
2	2	0.50 ± 0.13	$(7.22 \pm 2.27) \times 10^{-7}$	$(0.41 \pm 0.12) \times 10^{-7}$
	$X \pm$ S.D.	0.33 ± 0.23 [c]	$(5.09 \pm 2.98) \times 10^{-7}$ [c]	$(1.01 \pm 0.73) \times 10^{-7}$ [c]
10	1	0.17 ± 0.06	$(1.28 \pm 0.39) \times 10^{-6}$	$(8.96 \pm 2.98) \times 10^{-7}$
10	2	0.34 ± 0.11	$(2.27 \pm 0.74) \times 10^{-6}$	$(1.05 \pm 0.38) \times 10^{-7}$
	$X \pm$ S.D.	0.26 ± 0.14 [c]	$(1.78 \pm 0.82) \times 10^{-6}$ [c]	$(5.02 \pm 4.78) \times 10^{-7}$ [c]
50	1	0.16 ± 0.05	$(0.60 \pm 0.21) \times 10^{-5}$	$(4.02 \pm 1.25) \times 10^{-6}$
50	2	0.30 ± 0.09	$(0.96 \pm 0.29) \times 10^{-5}$	$(0.21 \pm 0.07) \times 10^{-6}$
	$X \pm$ S.D.	0.23 ± 0.12 [c]	$(0.78 \pm 0.32) \times 10^{-5}$	$(2.10 \pm 2.23) \times 10^{-6}$ [c]

[a] The modified Model B is Model B (epidermis-distribution model) with diffusion coefficient variation in epidermis. The epidermis was divided into two parts of equal thickness [near stratum corneum (Ns) and near dermis (Nd)]. The Nd-to-Ns diffusion coefficient ratios ($D_{2\beta,Nd}/D_{2\beta,Ns} = D_{1,Nd}/D_{1,Ns}$) were assigned values of 2, 10, and 50 for the two parts.
[b] Configuration 1: stratum corneum → epidermis → dermis; configuration 2: dermis → epidermis → stratum corneum.
[c] Significantly different.

tion of the diffusion coefficient in the epidermis is the best of all models.

Anatomical and biochemical basis of Model C. It has been shown that there are numerous enzyme systems beneath the stratum corneum in the viable epidermis capable of metabolizing drugs (Montagna, 1955, 1962; Weinstein et al., 1968; Bamshed, 1969; Laerum, 1969; Meyer and Neurand, 1976; Chapman et al., 1977; Yu et al., 1980a; Bickers et al., 1982). However, it has not been clear as to how the distribution of the enzymes might vary with epidermal depth. The enzyme activity appears to follow closely the presence of the mitochondria and ribosomes/endo-

TABLE 8

Examination of modified Model C with stripped skin experiments of $E_{2\beta}$: diffusion and metabolism parameters deduced from the modified Model C [a]

D_{Nd}/D_{Ns}	Configuration [b]	k (s^{-1})	$D_{2\beta,Nd}$ (cm^2/s)	$D_{1,Nd}$ (cm^2/s)
2	1	0.65 ± 0.26	$(5.05 \pm 1.89) \times 10^{-7}$	$(6.06 \pm 2.40) \times 10^{-7}$
2	2	0.69 ± 0.31	$(9.00 \pm 2.90) \times 10^{-7}$	$(2.00 \pm 0.79) \times 10^{-7}$
	$X \pm$ S.D.	0.67 ± 0.27	$(7.02 \pm 3.10) \times 10^{-7}$	$(4.03 \pm 2.89) \times 10^{-7}$ [c]
10	1	0.70 ± 0.28	$(2.03 \pm 0.81) \times 10^{-6}$	$(23.2 \pm 9.20) \times 10^{-7}$
10	2	0.69 ± 0.31	$(3.51 \pm 1.41) \times 10^{-6}$	$(7.03 \pm 2.80) \times 10^{-7}$
	$X \pm$ S.D.	0.70 ± 0.28	$(2.77 \pm 1.31) \times 10^{-6}$	$(15.1 \pm 11.5) \times 10^{-7}$ [c]
50	1	0.73 ± 0.26	$(1.90 \pm 0.67) \times 10^{-5}$	$(10.9 \pm 4.30) \times 10^{-6}$
50	2	0.78 ± 0.28	$(2.50 \pm 1.05) \times 10^{-5}$	$(3.70 \pm 1.38) \times 10^{-6}$
	$X \pm$ S.D.	0.76 ± 0.27	$(2.20 \pm 0.85) \times 10^{-5}$	$(7.30 \pm 5.15) \times 10^{-6}$ [c]

[a] The modified Model C is Model C (basal layer-distribution model) with diffusion coefficient variation in epidermis. The epidermis was divided into two parts of equal thickness [near stratum corneum (Ns) and near dermis (Nd)]. The Nd-to-Ns diffusion coefficient ratios ($D_{2\beta,Nd}/D_{2\beta,Ns} = D_{1,Nd}/D_{1,Ns}$) were assigned values of 2, 10, and 50 for the two parts.
[b] Configuration 1: stratum corneum → epidermis → dermis; configuration 2: dermis → epidermis → stratum corneum.
[c] Significantly different.

plasmic reticulum in the epidermis (Akin and Norred, 1976; Pohl et al., 1976). As epidermal cells are keratinized upward from the basal layer, they may lose their mitotic potential and general enzyme activity. Histochemical methods have shown that several enzymes, especially oxidase and dehydrogenase, are found in the basal cells and become progressively sparser in the spinous cells immediately above them (Louviere, 1956; Glenner, 1957; Burstone, 1959, 1960; Fand et al., 1959). Thus, Model C appears to be reasonable from the anatomical/biochemical standpoint.

Appendix A: Assessing the Error in Flux Measurement Caused by Permeant Retention in Skin Tissue

In the two-chamber diffusion cell experiments, when the volume of the receiver chamber (V_R) is small and the amount of permeant partitioning/binding into the skin tissue is large, a systematic error may occur in the fluxes determined by Eqns 1–3. The error arises because the amount of permeant retained in the skin tissue (stratum corneum, epidermis, and/or dermis) is not negligible compared to the amount of permeant in the receiver chamber. The important point here is that this error may be significant even when quasi-steady-state conditions are maintained; in all of the experiments in the present research, the permeant concentration in the donor chamber was held constant and the receiver chamber concentration was under essentially sink conditions ($\lesssim 10\%$ of the donor concentration).

Fig. 5 presents models that show how this error may be assessed for the permeant (e.g., constant concentration of $E_{2\beta}$ in the donor chamber) transport with single layer membrane (e.g., dermis), and with multiple layer membranes (e.g., stripped skin and full-thickness skin). The shaded area in Fig. 5 reflects the amount (ΔA) of permeant retained in the skin tissue. Since the permeant amount in the receiver chamber (A_R) is given by

$$A_R = C_R V_R \tag{A1}$$

where C_R and V_R are, respectively, the permeant

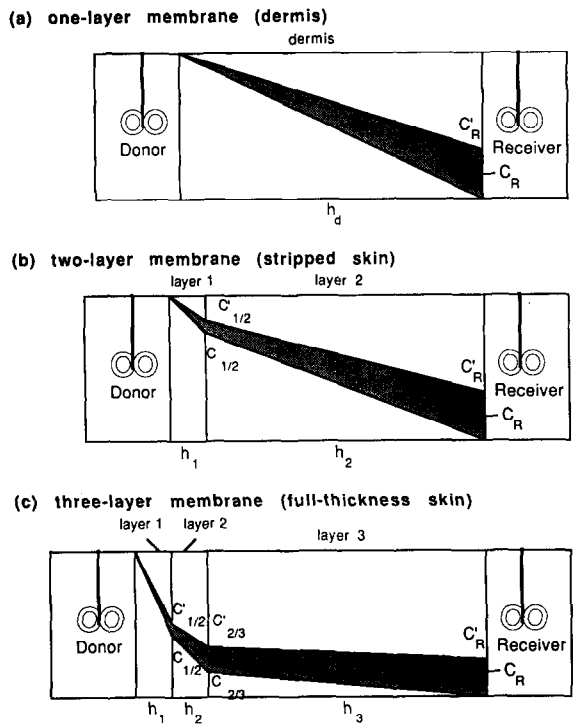

Fig. 5. Physical models for assessing the error in the flux determination caused by permeant retention in skin tissue in two-chamber diffusion cell experiments with (a) one-layer membrane (dermis), (b) two-layer membrane (stripped skin), and (c) three-layer membrane (full-thickness skin).

concentration and the solution volume in the receiver chamber, in the 'worst case' (i.e., no sampling/replacement in the receiver chamber), the ratio of the true flux, J_{true}, to the 'apparent' flux, J_{app}, is approximately given by

$$\frac{J_{true}}{J_{app}} = \frac{A_R + \Delta A}{A_R} \tag{A2}$$

For the case of a *one-layer membrane* such as dermis (Fig. 5a),

$$\Delta A = \frac{C'_R}{2} Sh_d = \frac{K C_R V_d}{2} \tag{A3}$$

where $K = C'_R/C_R$ is the apparent permeant partition coefficient for the membrane and the aqueous solution in the receiver chamber, and $V_d = Sh_d$, is the effective volume of the dermis and h_d is the thickness of the dermis. The ratio of the true flux,

J_{true}, to the apparent flux, J_{app}, is therefore given by

$$\frac{J_{true}}{J_{app}} = 1 + \frac{K\left(\frac{V_d}{V_R}\right)}{2} \tag{A4}$$

For the case of a *two-layer membrane* such as stripped skin (Fig. 5b), near linear gradients are assumed within the basal layer for mathematical simplicity. The fractional concentrations at the layer 1/layer 2 interface ($C'_{1/2}$ and $C_{1/2}$) are given by

$$C'_{1/2} = \frac{R_2 + C'_R R_1}{R_1 + R_2} \text{ and } C_{1/2} = \frac{R_2}{R_1 + R_2} \tag{A5}$$

where $R_1 = 1/P_1$ and $R_2 = 1/P_2$ may be termed the resistances to layers 1 and 2. The concentration build-up at the interface is proportional to that in the receiver chamber, i.e.,

$$C'_{1/2} - C_{1/2} = \frac{R_1}{R_1 + R_2} C'_R = \frac{R_1}{R_1 + R_2} KC_R \tag{A6}$$

Using the area equations for a triangle and a parallelogram, we obtain the amount of permeant retained in layers 1 (ΔA_1) and 2 (ΔA_2),

$$\Delta A_1 = \frac{(C'_{1/2} - C_{1/2})Sh_1}{2} = \frac{KC_R V_1}{2} \frac{R_1}{R_1 + R_2} \tag{A7}$$

$$\begin{aligned} \Delta A_2 &= \frac{\left[C'_R - (C'_{1/2} - C_{1/2})\right] Sh_2}{2} \\ &\quad + (C'_{1/2} - C_{1/2})Sh_2 \\ &= \frac{KC_R V_2}{2} \frac{R_2}{R_1 + R_2} + KC_R V_2 \frac{R_1}{R_1 + R_2} \\ &= KC_R V_2 \left(\frac{R_1 + R_2/2}{R_1 + R_2}\right) \end{aligned} \tag{A8}$$

where $V_1 = Sh_1$ and $V_2 = Sh_2$ are the effective volumes of layers 1 and 2 and h_1 and h_2 denote the thicknesses of layers 1 and 2, and hence we have immediately the total amount retained in the two-layer membrane ($\Delta A = \Delta A_1 + \Delta A_2$), and the ratio of the true flux, J_{true}, to the apparent flux, J_{app}, for the two-layer membrane case:

$$\begin{aligned} \frac{J_{true}}{J_{app}} &= 1 + \frac{\Delta A_1}{A_R} + \frac{\Delta A_2}{A_R} \\ &= 1 + K\left(\frac{V_1}{V_R}\right)\left(\frac{R_1/2}{R_1 + R_2}\right) \\ &\quad + K\left(\frac{V_2}{V_R}\right)\left(\frac{R_1 + R_2/2}{R_1 + R_2}\right) \end{aligned} \tag{A9}$$

In *configuration 1* experiments where epidermis (e) is layer 1 and dermis (d) layer 2, the true flux-to-apparent flux ratio is given by

$$\begin{aligned} \frac{J_{true}}{J_{app}} &= 1 + \frac{\Delta A_e}{A_R} + \frac{\Delta A_d}{A_R} \\ &= 1 + K\left(\frac{V_e}{V_R}\right)\left(\frac{R_e/2}{R_e + R_d}\right) \\ &\quad + K\left(\frac{V_d}{V_R}\right)\left(\frac{R_e + R_d/2}{R_e + R_d}\right) \end{aligned} \tag{A10}$$

Similarly, the true flux-to-apparent flux ratio is also obtained for *configuration 2* experiments where dermis (d) is layer 1 and epidermis (e) layer 2,

$$\begin{aligned} \frac{J_{true}}{J_{app}} &= 1 + \frac{\Delta A_d}{A_R} + \frac{\Delta A_e}{A_R} \\ &= 1 + K\left(\frac{V_d}{V_R}\right)\left(\frac{R_d/2}{R_d + R_e}\right) \\ &\quad + K\left(\frac{V_e}{V_R}\right)\left(\frac{R_d + R_e/2}{R_d + R_e}\right) \end{aligned} \tag{A11}$$

For the case of a *three-layer membrane* such as full-thickness skin (Fig. 5c) where $R_3 = 1/P_3$ and $V_3 = Sh_3$ are the resistance and the effective volume of layer 3, respectively, we may deduce, by

analogous reasoning, the following ratio of the true flux, J_{true} to the apparent flux, J_{app}

$$\frac{J_{true}}{J_{app}} = 1 + \frac{\Delta A_1}{A_R} + \frac{\Delta A_2}{A_R} + \frac{\Delta A_3}{A_R}$$

$$= 1 + K\left(\frac{V_1}{V_R}\right)\left(\frac{R_1/2}{R_1 + R_2 + R_3}\right) + K\left(\frac{V_2}{V_R}\right)\left(\frac{R_1 + R_2/2}{R_1 + R_2 + R_3}\right) + K\left(\frac{V_3}{V_R}\right)\left(\frac{R_1 + R_2 + R_3/2}{R_1 + R_2 + R_3}\right) \quad \text{(A12)}$$

Therefore, the true flux-to-apparent flux ratio is obtained for *configuration 1* experiments where the order of layers is stratum corneum (s), epidermis (e), and dermis (d)

$$\frac{J_{true}}{J_{app}} = 1 + \frac{\Delta A_s}{A_R} + \frac{\Delta A_e}{A_R} + \frac{\Delta A_d}{A_R}$$

$$= 1 + K\left(\frac{V_s}{V_R}\right)\left(\frac{R_s/2}{R_s + R_e + R_d}\right) + K\left(\frac{V_e}{V_R}\right)\left(\frac{R_s + R_e/2}{R_s + R_e + R_d}\right) + K\left(\frac{V_d}{V_R}\right)\left(\frac{R_s + R_e + R_d/2}{R_s + R_e + R_d}\right) \quad \text{(A13)}$$

Similarly, the true flux-to-apparent flux ratio is obtained for *configuration 2* experiments where the order of layers is dermis (d), epidermis (e), and stratum corneum (s)

$$\frac{J_{true}}{J_{app}} = 1 + \frac{\Delta A_d}{A_R} + \frac{\Delta A_e}{A_R} + \frac{\Delta A_s}{A_R}$$

$$= 1 + K\left(\frac{V_d}{V_R}\right)\left(\frac{R_d/2}{R_d + R_e + R_s}\right) + K\left(\frac{V_e}{V_R}\right)\left(\frac{R_d + R_e/2}{R_d + R_e + R_s}\right) + K\left(\frac{V_s}{V_R}\right)\left(\frac{R_d + R_e + R_s/2}{R_d + R_e + R_s}\right) \quad \text{(A14)}$$

In terms of permeability coefficients, we may write

$$\frac{P_{true}}{P_{app}} = \frac{J_{true}}{J_{app}} \quad \text{(A15)}$$

and this would apply to dermis (Eqn A4), stripped skin (Eqns A10 and A11), and full-thickness skin (Eqns A13 and A14).

The term, $K(V_d/V_R)$ may be determined as

$$K\left(\frac{V_d}{V_R}\right) = \left(\frac{A_d}{A_{aq}}\right)_{eq} \quad \text{(A16)}$$

where $(A_d/A_{aq})_{eq}$ represents the ratio of amount of permeant partitioned between the skin membrane and the aqueous solution at equilibrium. The ratios were experimentally determined when the pieces of epidermis/dermis were equilibrated in 2 ml pure saline solution. The amount ratios, A_d/A_{aq} (about 0.50), or the respective apparent binding/partition coefficients, K (about 50), were found to be essentially the same for $E_{2\beta}$ and E_1 (Liu, 1989). In a preliminary experiment, the $E_{2\beta}$ apparent binding/partition coefficient, K, for stratum corneum was found to be comparable to that for dermis.

Table 9 summarizes and compares the true flux-to-apparent flux ratios in several situations. Eqns A4, A10, A11, A13 and A14 were used in the calculations with the permeability coefficients (Table 4) for the resistance values (R_s, R_e, and R_d), the thickness values ($h_s = 20$, $h_e = 20$, and $h_d = 250$ μm), and the effective diffusion area ($S = 0.7$ cm^2). The apparent partition/binding coefficient ($K = 50$) was assumed to be the same for dermis, epidermis, and stratum corneum. As can be seen in Table 9, dermis layer with its relatively larger volume, V_d, dominates the total retained amount in the skin tissue, and the problem of permeant retention in skin tissue is less important in configuration 2 situations.

Two kinds of diffusion experiments (configuration 1) (Methods A and B) were also conducted with two pieces of skin from the same mouse. Method A is described in Materials and Methods and a sampling volume (with replacement) of 0.1 ml was used for eight data points after steady

TABLE 9

The relative retained amounts ($\Delta A/A_R$) and the true flux-to-apparent flux ratios (J_{true}/J_{app}) for different skin membrane components and experimental configurations [a]

Membrane	Configuration	$\Delta A_d/A_R$	$\Delta A_e/A_R$	$\Delta A_s/A_R$	J_{true}/J_{app}
Dermis		0.219			1.22
Stripped skin	configuration 1 (e → d)	0.293	0.00587		1.30
Stripped skin	configuration 2 (d → e)	0.147	0.0293		1.18
Full-thickness skin	configuration 1 (s → e → d)	0.409	0.0289	0.0138	1.45
Full-thickness skin	configuration 2 (d → e → s)	0.0314	0.00629	0.0214	1.06

[a] Calculations were carried out with Eqns A4 (for dermis), A10 and A11 (for stripped skin), and A13 and A14 (for full-thickness skin).

state was reached and this situation approximates the worst case (i.e., the J_{app} in Eqns A4, A10, A11, A13 and A14). In Method B, a sampling volume (with replacement) of 1.5 ml was used and a plateau was attained in the sampled amount vs time plot, this corresponding to J_{true}. Theoretical simulation for Method A was carried out (i.e., the P_{app} was calculated from only the amount appearing in the receiver chamber with a sampling/replacing volume of 0.1 ml for eight times after the steady state). Table 10 presents the results of a validation study of Eqns A10 and A13 using Eqns A15 and A16. The experimental P_{true}/P_{app} values agree reasonably well with the predicted values based upon Eqns A10 and A13. Also, these results provide correction factors for flux values obtained using Eqns 1–3.

A final important aspect here is to evaluate how accurate the simple approach is, where the linear approximation in the concentration-distance profiles was made in the quasi-steady state. Taking the dermis case as an example, a full numerical analysis with non-steady state approach was carried out accounting for the simultaneous diffusion and immobilized retention of $E_{2\beta}$ in the dermis. The results demonstrate that the simple quasi-steady-state approach provides a good approximation (within 10% deviation) to the more rigorous but complicated non-steady-state approach after two lag times.

TABLE 10

Assessing the error in the flux determination caused by the permeant retention in the skin tissue: comparison of the two kinds of experiments and theoretical predictions

Skin	Permeant	P value (cm/s) ($\times 10^6$) [a]		P_{true}/P_{app}		
		P_{true}	P_{app}	Experiment	Method A simulation [b]	Eqn A10 Eqn A13 [c]
Stripped skin	$E_{2\beta}$	41.0 ± 22.8	34.1 ± 3.70	1.20 ± 0.45	1.25 ± 0.07	1.30 ± 0.08
	E_1	49.0 ± 14.4	37.5 ± 3.70	1.31 ± 0.33	1.25 ± 0.07	1.30 ± 0.08
Full-thickness skin	$E_{2\beta}$	5.96 ± 2.08	3.89 ± 1.10	1.53 ± 0.16	1.41 ± 0.14	1.45 ± 0.16
	E_1	9.19 ± 2.94	6.46 ± 1.22	1.43 ± 0.32	1.41 ± 0.14	1.45 ± 0.16

[a] Two-chamber cell (configuration 1) experiments were conducted with two pieces of skin from the same mouse using two procedures (Methods A and B). In Method A, a sampling volume of 0.1 ml was used for eight times after the steady state and this situation approximates the worst case (i.e., the P_{app} in Eqns A10 and A13). In Method B, a sampling volume of 1.5 ml was used and a plateau was attained in the sampled amount vs time plot, this corresponding to P_{true}. The P values, calculated from the normalized total forward fluxes, are expressed as the mean ± S.D. ($n = 3$).

[b] Theoretical simulation for Method A.

[c] Theoretical prediction for the worst case (i.e., the P_{app} in Eqns A10 and A13 with no sampling) with $A_d/A_{aq} = 0.50 \pm 0.16$.

Appendix B: Mathematical Methods for Solving the Diffusion-Metabolism Equations

Analytical solution

Eqns 5–8 were solved simultaneously for the simultaneous diffusion and metabolism of A (permeant/substrate) → B (metabolite) (Yu et al., 1980b). The solution can be written in matrix form for the i-th layer as:

$$\begin{bmatrix} A(x_i) \\ J_A(x_i) \\ B(x_i) \\ J_B(x_i) \end{bmatrix} = \begin{bmatrix} \cosh(a_i\Delta x) & -\dfrac{\sinh(a_i\Delta x)}{a_i D_{A,i}} & 0 & 0 \\ -a_i D_{A,i}\sinh(a_i\Delta x) & \cosh(a_i\Delta x) & 0 & 0 \\ \dfrac{D_{A,i}}{D_{B,i}}[1-\cosh(a_i\Delta x)] & \dfrac{\sinh(a_i\Delta x)-a_i\Delta x}{a_i D_{B,i}} & 1 & -\dfrac{\Delta x}{D_{B,i}} \\ a_i D_{A,i}\sinh(a_i\Delta x) & 1-\cosh(a_i\Delta x) & 0 & 1 \end{bmatrix} \begin{bmatrix} C_A(x_{i-1}) \\ J_A(x_{i-1}) \\ C_B(x_{i-1}) \\ J_B(x_{i-1}) \end{bmatrix} \tag{B1}$$

where

$$a_i = \sqrt{\frac{k_i}{D_{A,i}}} \tag{B2}$$

$$\Delta x = x_i - x_{i-1} \tag{B3}$$

For the homogeneous enzyme layer (i.e., epidermis in Model B or the basal cell layer in Model C) with thickness $\Delta x = h$, the solution may be written in terms of fluxes as:

$$J_{2\beta,f} = aD_{2\beta}\left[\operatorname{csch}(ah)C_{2\beta,l} - \coth(ah)C_{2\beta,r}\right] \tag{B4}$$

$$J_{1,f} = \frac{D_{2\beta}}{h}(C_{2\beta,l} - C_{2\beta,r}) + \frac{D_1}{h}(C_{1,l} - C_{1,r}) - aD_{2\beta}\left[\operatorname{csch}(ah)C_{2\beta,l} - \coth(ah)C_{2\beta,r}\right] \tag{B5}$$

$$J_{1,b} = -\frac{D_{2\beta}}{h}(C_{2\beta,l} - C_{2\beta,r}) - \frac{D_1}{h}(C_{1,l} - C_{1,r}) + aD_{2\beta}\left[\coth(ah)C_{2\beta,l} - \operatorname{csch}(ah)C_{2\beta,r}\right] \tag{B6}$$

$$J_{1,f} + J_{1,b} = aD_{2\beta}\left\{\left[\coth(ah) - \operatorname{csch}(ah)\right] \times (C_{2\beta,l} + C_{2\beta,r})\right\} \tag{B7}$$

$$J_{2\beta,f} + J_{1,f} + J_{1,b} = aD_{2\beta}\left[\coth(ah)C_{2\beta,l} - \operatorname{csch}(ah)C_{2\beta,r}\right] \tag{B8}$$

where $C_{2\beta,l}$, $C_{2\beta,r}$, and $C_{1,l}$, $C_{1,r}$ are the concentrations of $E_{2\beta}$ (permeant/substrate) and E_1 (metabolite) at the left and right sides of the enzyme layer, respectively.

Three parameters ($D_{2\beta}$, D_1, and k) may be deduced providing the three experimental fluxes ($J_{2\beta,f}$, $J_{1,f}$ and $J_{1,b}$) and boundary concentrations (Eqns 11 and 12).

Numerical approach

Eqns 5 and 6 were also solved numerically by mathematically dividing the enzyme layer into n (e.g., 10) equally thick compartments of $\Delta x = h/10$ in width (Hsu, 1981). The subscripts l and r represent the surface of the enzyme layer at the left and right sides, and the subscripts $1, 2, \ldots, 10$ correspond to compartments $1, 2, \ldots, 10$, respectively.

For compartment 1:

$$\frac{D_{2\beta}}{\Delta x}\left[\frac{(C_{2\beta,2} - C_{2\beta,1})}{\Delta x} - \frac{(C_{2\beta,1} - C_{2\beta,l})}{\frac{\Delta x}{2}}\right] - kC_{2\beta,1} = 0 \tag{B9}$$

$$\frac{D_1}{\Delta x}\left[\frac{(C_{1,2} - C_{1,1})}{\Delta x} - \frac{(C_{1,1} - C_{1,l})}{\frac{\Delta x}{2}}\right] + kC_{2\beta,1} = 0 \tag{B10}$$

For compartment n ($n = 2$–9):

$$\frac{D_{2\beta}}{\Delta x}\left[\frac{(C_{2\beta,n+1} - C_{2\beta,n})}{\Delta x} - \frac{(C_{2\beta,n} - C_{2\beta,n-1})}{\Delta x}\right] - kC_{2\beta,n} = 0 \quad \text{(B11)}$$

$$\frac{D_1}{\Delta x}\left[\frac{(C_{1,n+1} - C_{1,n})}{\Delta x} - \frac{(C_{1,n} - C_{1,n-1})}{\Delta x}\right] + kC_{2\beta,n} = 0 \quad \text{(B12)}$$

For compartment 10:

$$\frac{D_{2\beta}}{\Delta x}\left[\frac{(C_{2\beta,r} - C_{2\beta,10})}{\frac{\Delta x}{2}} - \frac{(C_{2\beta,10} - C_{2\beta,9})}{\Delta x}\right] - kC_{2\beta,10} = 0 \quad \text{(B13)}$$

$$\frac{D_1}{\Delta x}\left[\frac{(C_{1,r} - C_{1,10})}{\frac{\Delta x}{2}} - \frac{(C_{1,10} - C_{1,9})}{\Delta x}\right] + kC_{2\beta,10} = 0 \quad \text{(B14)}$$

Three parameters ($D_{2\beta}$, D_1, and k) may be deduced with the following flux expressions providing the three experimental fluxes ($J_{2\beta,f}$, $J_{1,f}$, and $J_{1,b}$) and boundary concentrations (Eqns 11 and 12):

$$J_{2\beta,f} = \frac{D_{2\beta}}{\frac{\Delta x}{2}}(C_{2\beta,10} - C_{2\beta,r}) \quad \text{(B15)}$$

$$J_{1,f} = \frac{D_1}{\frac{\Delta x}{2}}(C_{1,10} - C_{1,r}) \quad \text{(B16)}$$

$$J_{1,b} = -\frac{D_1}{\frac{\Delta x}{2}}(C_{1,1} - C_{1,1}) \quad \text{(B17)}$$

$$J_{2\beta,f} + J_{1,f} + J_{1,b} = \frac{D_{2\beta}}{\frac{\Delta x}{2}}(C_{2\beta,1} - C_{2\beta,1}) \quad \text{(B18)}$$

Acknowledgements

This research was supported by the Ciba-Geigy Corp. (Ardsley, NY). P.L. was supported in part by the University of Utah Graduate Research Fellowship (1987–1988). Appreciation is expressed to Drs Bradley D. Anderson and Raymond E. Galinsky for help on HPLC assay development.

References

Akin, F.J. and Norred, W.P., Factors affecting measurement of aryl hydrocarbon hydroxylase activity in mouse skin. *J. Invest. Dermatol.*, 67 (1976) 709–712.

Ando, H.Y., Ho, N.F.H. and Higuchi, W.I., Skin as an active metabolizing barrier I. theoretical analysis of topical bioavailability. *J. Pharm. Sci.*, 66 (1977) 1525–1528.

Bamshad, J., Catechol-*o*-methyl transferase in epidermis, dermis and whole skin. *J. Invest. Dermatol.*, 52 (1969) 351–352.

Bickers, D.R., Dutta-Choudhury, T. and Mukhtar, H., Epidermis: a site of drug metabolism in neonatal rat skin. Studies on cytochrome P-450 content and mixed-function oxidase and epoxide hydrolase activity. *Mol. Pharmacol.*, 21 (1982) 239–247.

Bucks, D.A.W., Skin structure and metabolism: relevance to the design of cutaneous therapeutics. *Pharm. Res.*, 4 (1984) 148–153.

Burstone, M.S., New histochemical technique for the demonstration of tissue oxidase (cytochrome oxidase). *J. Histochem. Cytochem.*, 7 (1959) 112–122.

Burstone, M.S., Histochemical demonstration of cytochrome oxidase with new amino reagents. *J. Histochem. Cytochem.*, 7 (1960) 63–70.

Chapman, P.H., Rawlins, M.D. and Shuster, S., Aryl hydroxylase in adult human skin. *Br. J. Clin. Pharmacol.*, 4 (1977) 644–650.

Davis, B.P., Rampini, E., and Hsia, S.L., 17β-hydroxysteroid dehydrogenase of rat skin, substrate specificity and inhibitors. *J. Biol. Chem.*, 247 (1972) 1407–1413.

Durrheim, H., Flynn, G.L., Higuchi, W.I. and Bell, C.R., Permeation of hairless mouse skin. I. experimental methods and comparison with human epidermal permeation by alkanols. *J. Pharm. Sci.*, 69 (1980), 781–786.

Fand, S.B., Levine, H.L. and Erwin, H.L., A reappraisal of the histochemical method for carbonic anhydrase. *J. Histochem. Cytochem.*, 7 (1959) 27–33.

Farber, E. and Louvere, C.D., Histochemical localization of specific oxidative enzymes. IV. Soluble oxidation-reduction dyes as aids in the histochemical localization of oxidative enzymes with tetrazolium salts. *J. Histochem. Cytochem.*, 4 (1956) 347–356.

Finnen, M.J., Herdman, M.L. and Shuster, S., Distribution and subcellular localization of drug metabolizing enzymes in the skin. *Br. J. Dermatol.*, 113 (1985) 713–721.

Frost, P., Weinstein, G.D. and Hsia, S.L., Metabolism of estradiol-17β and estrone in human skin. *J. Invest. Dermatol.*, 46 (1966), 584–585.

Ghanem, A.H., Mahmoud, H., Higuchi, W.I., Rohr, U.D., Borsadia, S., Liu, P., Fox, J.L. and Good, W.R., The effects of ethanol on the transport of β-estradiol and other permeants in hairless mouse skin. II. A new quantitative approach. *J. Cont. Rel.*, 6 (1987) 75–83.

Glenner, C.G., Burtner, H.J. and Brown, G.W. Jr, The histochemical demonstration of monoamine oxidase activity by tetrazolium salts. *J. Histochem. Cytochem.*, 5 (1957) 591–600.

Hsu, C.-C., Prodrug-based topical vaginal drug delivery: a physical model approach to simultaneous membrane transport and bioconversion. Ph.D. Thesis, The University of Michigan, Ann Arbor, MI (1981).

Kao, J. and Hall, J., Skin absorption and cutaneous first pass metabolism of topical steroid: in vitro studies with mouse in organic culture. *J. Pharmacol. Exp. Ther.*, 241 (1987) 482–487.

Laerum, O.D., Oxygen consumption of basal and differentiating cells from hairless mouse epidermis. *J. Invest. Dermatol.*, 52 (1969) 204–221.

Lee, G.J.-L., Carlson, R.M.K. and Kushinsky, S., Use of organic modifiers in the mobile phase for the reversed-phase high-performance liquid chromatographic separation of steroidal hormones. *J. Chromatogr.*, 212 (1981) 108–114.

Liu, P., Higuchi, W.I. and Good, W.R., Dermal/transdermal metabolism of β-estradiol in hairless mouse skin in vitro. Abstr. No. 47, PDD Section, *AAPS 1st Annual Meeting*, Washington, DC, November 1986.

Liu, P., The influences of ethanol on simultaneous diffusion and metabolism of β-estradiol in skin, Ph.D. Thesis, The University of Utah, Salt Lake City, UT (1989).

Longcope, C. and Williams, K.I.H., The metabolism of estrogens in normal women after pulse injections of ^{3}H-estradiol and ^{3}H-estrone. *J. Clin. Endocrinol. Metab.*, 38 (1974) 602–610.

Longcope, C., The metabolism of estrogens by human skin. In Mauvais-Jarvis, P., Vickers, C.F.H. and Wepierre, J. (Eds), *Percutaneous Absorption of Steroids*, Academic Press, New York, 1980, pp. 89–98.

Martin, R.J., Denyer, S.P. and Hadgraft, J., Skin metabolism of topically applied compounds. *Int. J. Pharm.*, 39 (1987) 23–32.

Meyer, W. and Neurand, K., The distribution of enzyme in the skin of the domestic pig. *Lab. Animals*, 10 (1976) 237–247.

Montagna, W., Histology and cytochemistry of human skin. IX. The distribution of non-specific esterase. *J. Biophys. Biochem. Cytol.*, 1 (1955) 13–16.

Montagna, W., *The Structure and Function of Skin*, Academic Press, New York, 1962, p. 46.

Noonan, P.K. and Wester, R.C., Cutaneous biotransformation: some pharmacological and toxicological implications. In Kydonieus, A.F. and Berner, B. (Eds), *Transdermal Delivery of Drugs*, Vol. I, CRC Press, Boca Raton, FL, 1987, p. 65.

Noonan, P.K. and Wester, R.C., Cutaneous metabolism of xenobiotics. In Marzulli, F.N. and Maibach, H.I. (Eds), *Dermatoxicology*, Hemisphere, New York, 1983, p. 71.

Pohl, R.J., Philpot, R.M. and Fonts, J.R., Cytochrome P-450 content and mixed-function oxidase activity in microsome isolated from mouse skin. *Drug Metab. Dispos.*, 4 (1976) 442–450.

Weinstein, G.D., Frost, P. and Hsia, S.L., In vitro interconversion of estrone and 17β-estradiol in human skin and vaginal mucosa. *J. Invest. Dermatol.*, 51 (1968) 4–10.

Yu, C.D., Fox, J.L., Ho, N.F.H. and Higuchi, W.I., Physical model evaluation of topical prodrug delivery – simultaneous transport and bioconversion of vidarabine-5′-valerate I. Physical model development. *J. Pharm. Sci.*, 68 (1979a) 1341–1346.

Yu, C.D., Fox, J.L., Ho, N.F.H. and Higuchi, W.I., Physical model evaluation of topical prodrug delivery – simultaneous transport and bioconversion of vidarabine-5′-valerate II. Parameter determination. *J. Pharm. Sci.*, 68 (1979b) 1347–1357.

Yu, C.D., Fox, J.L., Higuchi, W.I. and Ho, N.F.H., Physical model evaluation of topical prodrug delivery – simultaneous transport and bioconversion of vidarabine-5′-valerate IV. Distribution of esterase and deaminase enzyme in hairless mouse skin. *J. Pharm. Sci.*, 69 (1980a) 772–775.

Yu, C.D., Gordon, N.A., Fox, J.L., Ho, N.F.H. and Higuchi, W.I., Physical model evaluation of topical prodrug delivery – simultaneous transport and bioconversion of vidarabine-5′-valerate V. Mechanistic analysis of influence on non-homogeneous enzyme distribution in hairless mouse skin. *J. Pharm. Sci.*, 69 (1980b) 775–780.